Trans Indian Inst Met (2017) 70(3):631–637
DOI 10.1007/s12666-017-1089-7

TECHNICAL PAPER

# A Study on Microstructure, Texture and Precipitation Evolution at Different Stages of Steel Processing in Interstitial Free High Strength Steels

**Gaurav Bhargava**[1] · **Latimuni Patra**[1] · **Shrikant Pai**[1] · **Devasish Mishra**[1]

Received: 7 January 2017 / Accepted: 13 February 2017 / Published online: 3 March 2017


**Abstract** The formability characteristics of interstitial free high strength (IFHS) steels are significantly governed by processing parameters of steel at consecutive processing stages, chiefly hot rolling of slabs followed by cold reduction of hot rolled coils and finally annealing treatment of cold reduced coils. The present work focuses on investigating the steel processing parameters for a chosen set of processing parameters which in turn influence the final formability of the steel. The underlying objective is to study the effect of steel processing parameters, which in turn favorably control texture, microstructure, precipitate morphology and its distribution at each step to impart desired properties in the steel sheet in the end. In the current work, an IFHS steel chemistry is chosen with an objective to evaluate the contribution of texture, microstructure and precipitates generated at each processing step to the formability in relation with the chosen processing parameters.

**Keywords** Interstitial free high strength steel · Formability · Microstructure · Texture · Precipitate

**Abbreviations**

| | |
|---|---|
| IFHS | Interstitial free steel |
| RD | Rolling direction |
| ND | Normal direction |
| TD | Transverse direction |
| El% | Elongation percentage |
| r-Bar | Mean plastic strain ratio |
| Δr | Plastic anisotropy ratio |
| HR | Hot rolling (process/coil) |
| CR | Cold rolling (process/coil) |
| SRT | Slab reheating temperature |
| RDT | Roughing deformation temperature |
| CT | Coiling temperature |
| LHF | Ladle reheating furnace |
| RH | Ruhrstahl–Heraeus degasser |

✉ Gaurav Bhargava
gaurav.bhargava@jsw.in

1 JSW Steel Limited, Vijayanagar Works, Toranagallu, Karnataka 58327, India

## 1 Introduction

Interstitial free high strength (IFHS) steels due to their excellent formability and non-aging characteristics are widely preferred material for automotive applications. The characteristic sheet formability is quantified by high uniform elongation (%El), a high deep drawability ratio (r-Bar) and an optimum planar anisotropy ratio (Δr). For IFHS steels, to ensure such properties, a preferential {111} parallel to normal direction (ND) (or γ-Fiber—{111}//ND) texture is favorable (Fig. 1).

The understanding of the microstructural and textural evolution at each step of the processing stages is of utmost importance to improve sheet quality in terms of its deep-drawing properties [1]. A schematic diagram depicting an overall steel processing route of IFHS steel is shown in Fig. 2 which illustrates the conventional process that is followed for processing IFHS steel through continuous annealing route. Firstly, slabs with a defined control of chemistry are produced through continuous casting route, are subjected to hot rolling process.

A typical IFHS steel hot rolling (HR) processing can be subdivided into four sub processes, such as reheating, roughing, finishing rolling and controlled cooling. The first

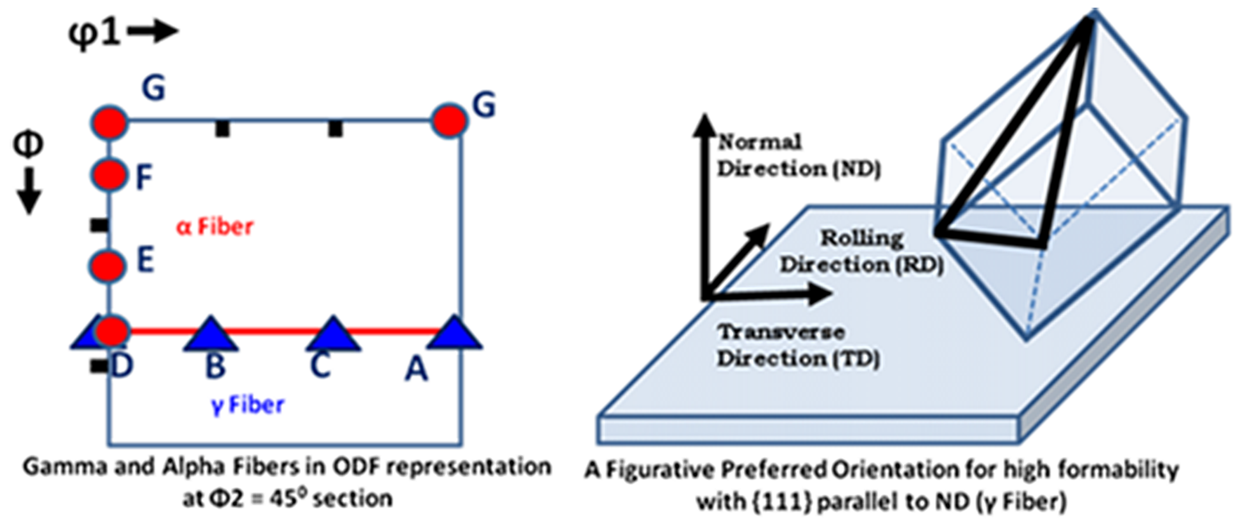


**γ Fiber**

| Slip System | φ1 | Φ | φ2 | $\bar{r}$ value |
|---|---|---|---|---|
| A (111)[-1 -1 2] | 90 | 54.7 | 45 | 2.6 |
| B (111)[1 -2 1] | 30 | 54.7 | 45 | 2.6 |
| C (111)[0 -1 1] | 60 | 54.7 | 45 | 2.6 |
| D (111)[1 -1 0] | 0 | 54.7 | 45 | 2.6 |

**α Fiber**

| Slip System | φ1 | Φ | φ2 | $\bar{r}$ value |
|---|---|---|---|---|
| D (111)[-1 -1 0] | 0 | 54.7 | 45 | 2.6 |
| E (112)[1 -1 0] | 0 | 35.3 | 45 | 2.1 |
| F (111)[0 -1 1] | 0 | 19.5 | 45 | 2.6 |
| G (111)[1 -1 0] | 0 | 54.7 | 45 | 2.6 |

**Fig. 1** Gamma and Alpha fiber representation

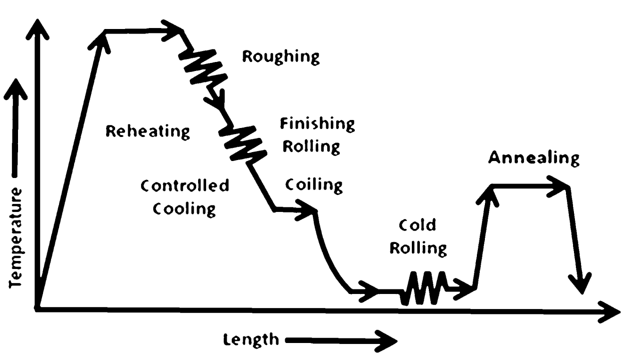


**Fig. 2** Schematic representation for steel processing route for IFHS steel

step, reheating is accomplished to promote homogenization and dissolution of dendritic structure. Slabs are soaked in a reheating furnace at a slab reheating temperature (SRT) for a certain period of time. Micro-alloying precipitates formed during and after solidification as the steel are subjected to continuous casting; dissolve either fully or partially during slab reheating. During slab reheating, the austenite grain growth behavior is affected by the presence of micro-alloy carbides/nitrides/carbonitrides which restricts the austenite grain growth [2]. It has been reported that localized and/or partial dissolution of micro-alloy carbides/carbonitrides/nitrides may lead to inhomogeneous austenite grain growth during reheating stage [2].

Afterwards, roughing of the slab is carried out in roughing mill to reduce the thickness of slab, in addition to breaking of scales before and after roughing using hydraulic scale breaker. This process is majorly controlled by roughing deformation temperature (RDT). Roughing deformation is carried out at a high temperature, where recrystallization is fast whereas micro alloy additions are still kept in solution. Subsequently, finish rolling is performed in order to achieve required HR thickness in rolling operation and conducted within a specific temperature range. This process is chiefly controlled by hot rolling finishing temperature (FRT). Finish rolling is carried out by rolling the preceding material through a multi-pass rolling mill. The rolling is usually conducted at lower temperatures than the earlier processes. Owing to low temperatures, the metal does not recrystallize between the passes [3].

Finally the finished rolled HR coil is subjected to controlled cooling treatment at run out table. Cold reduction process is carried out on HR coil, in which HR coil is rolled through a multipass mill at temperatures below the recrystallization temperature of the steel. The cold rolling process leads to increase in the yield strength and hardness of the steel coil. This operation is mainly done to achieve final required thickness as well as a close dimensional control. The full hard cold rolled coil is then subjected through annealing, a heat treatment process which is generally performed above recrystallization temperature that alters the physical properties and sometimes chemical redistribution of a material through phase transformation to increase its ductility and reduce its hardness, making it more formable.

## 2 Experimental

The experimental work has been divided into two parts: the steel processing and its simultaneous characterization which were concurrently done at each steel processing step:

### 2.1 Steel Making and Processing

For the present study a Ti and P based IFHS chemistry was chosen. The basic chemistry has been listed in the Table 1. The starting basic chemistry was produced from the hot metal which was subjected to de-sulphurization followed by basic oxygen furnace and alloy addition in ladle heating furnace (LHF). This was followed by interstitial elements (C, N, H, O) removal through Ruhrstahl–Heraeus (RH) degasser. The steel was casted into slab with a super heat of 30 °C having 220 mm thickness. The steel sample used in this investigation possessed standard chemistry.

Finishing temperature was set above 900 °C with a coiling temperature at 630 ± 15 °C. For hot rolling process, the process parameters for the sub processes such as slab reheating temperature, finish rolling temperature and coiling temperature are mentioned as in Table 2.

The hot rolled coils were then subjected to cold reduction and finally continuous annealing at hot dip galvanizing line. The parameters for the above mentioned process are mentioned in Table 3. A cold reduction of 75% was provided to hot rolled coils, after removal of oxide layer film by pickling process. To achieve final properties, the cold rolled coil was annealed at a temperature of 780 ± 15 °C. To provide material corrosion resistance, galvanizing treatment in continuous galvanizing line was performed.

**Table 1** Chemical composition (in wt%) of IFHS steel

| Material name | C | Mn | Al | N | Ti | P |
|---|---|---|---|---|---|---|
| IFHS | 0.002 | 0.36 | 0.05 | 0.0036 | 0.033 | 0.052 |

**Table 2** Hot rolling process parameters

| Material name | SRT (°C) | FT (°C) | CT (°C) |
|---|---|---|---|
| IFHS | 1020 | 907 | 631 |

**Table 3** Cold rolling and annealing process parameters

| Material name | Reduction (%) | Annealing temp (°C) |
|---|---|---|
| IFHS | 80 | 785 |

### 2.2 Material Characterization

The steel substrate was characterized at each processing step starting with mechanical properties, grain size measurement and precipitate characterization using energy-dispersive X-ray spectroscopy (EDS). From the same substrate, set of samples at different stages of processing were chosen for the above mentioned characterization. After end of processing step (i.e. after hot rolling, cold rolling and annealing) sampling was done precisely from the locations wherein the process parameters exactly matched the predefined values for processing.

For mechanical testing, the samples of 80 mm gauge length and width of 20 mm were prepared and mechanically tested according to EN 10002-1 standard. Samples were tested in three directions: longitudinal (L), transverse (T) and diagonal (D) direction with respect to rolling direction of sample. For microstructural and precipitation analysis, samples were polished and etched in 4% Nital solution. Microstructural evaluation was done using optical microscope of Zeiss model AXIOVERT 40MAT under the magnification of 100×. For grain size evaluation, line intercept method was used. For precipitation analysis, energy-dispersive X-ray spectroscopy (EDS) in scanning electron microscope (SEM) of JEOL, HITACHI Model S-3400 N was used. A resolution of 5000× and secondary electron mode was used for precipitation analysis. Bulk texture measurements were carried out using X-ray diffraction technology of Philips XPERT Theta–Theta Diffractometer.

## 3 Results and Discussion

### 3.1 Mechanical Characterization of Steel

Table 4 lists the mechanical properties of the steel at each steel processing step. The mechanical properties have been tested in both longitudinal (L) and transverse direction (T) to that of rolling direction for hot rolled, cold rolled and annealed samples.

**Table 4** Mechanical Characterization of IFHS Steel

| Material | Sample direction | YS | UTS | EL% | n Value | r Bar | Δr | Mean grain size |
|---|---|---|---|---|---|---|---|---|
| Hot rolled IFHS | L | 255 | 364 | 40.2 | 0.249 | – | – | 11.5 |
| | T | 280 | 373 | 34.2 | 0.231 | – | – | |
| Cold rolled IFHS | L | 740 | 755 | 1.96 | – | – | – | 7 |
| | T | 818 | 842 | 1.24 | – | – | – | |
| Annealed IFHS | L | 226 | 372 | 39 | 0.21 | 1.56 | 0.13 | 9.5 |
| | D | 239 | 369 | 40 | 0.21 | | | |
| | T | 241 | 368 | 37 | 0.21 | | | |

### 3.2 Microstructural and Precipitation Analysis

Figures 3 and 4 show the characterization of microstructure and precipitates at different stages of steel processing. Figure 3a, b, c shows the evolution of final annealed microstructure from the hot rolled microstructure. The evolution of various precipitates at various stages of steel processing is shown in the Fig. 4a, b, c.

### 3.3 Texture Measurement

Pole figure is the graphical representation of the orientation of objects in space. It is used to represent the orientation distribution of crystallographic lattice planes. The complete information about the texture can be found by using crystal orientation map commonly called orientation distribution function (ODF) map. This map describes the frequency of particular orientation in a 3D space called as Euler space. Three Euler angle φ1, ϕ, φ2 are the set of consecutive rotation given to each crystallite that merges the crystallographic axes into specimen axis. Figure 5 shows the pole figure and ODF of material at different stages of processing.

In a normal steel processing route for manufacturing IFHS steels, conventionally, hot rolling of continuous cast slabs is carried out in the austenite range followed by cold rolling reduction (75–80%) and a subsequent batch or continuous annealing for recrystallization (Fig. 1).

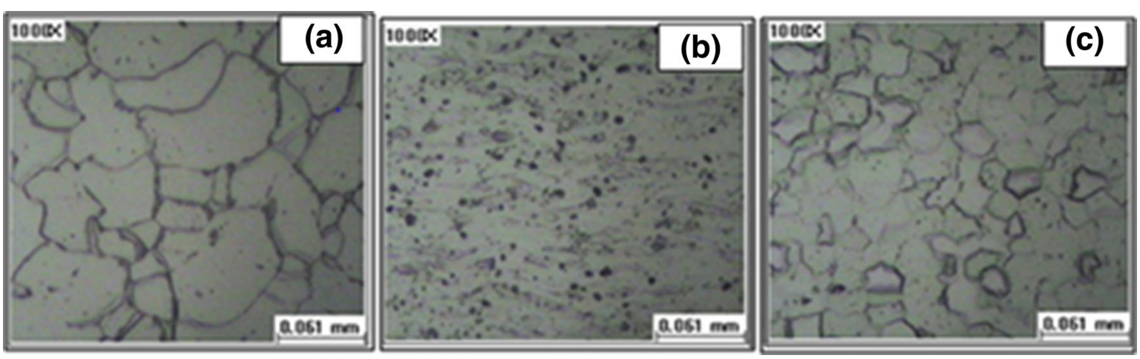


**Fig. 3** Microstructural evolution in **a** hot rolled **b** cold rolled **c** annealed IFHS steel

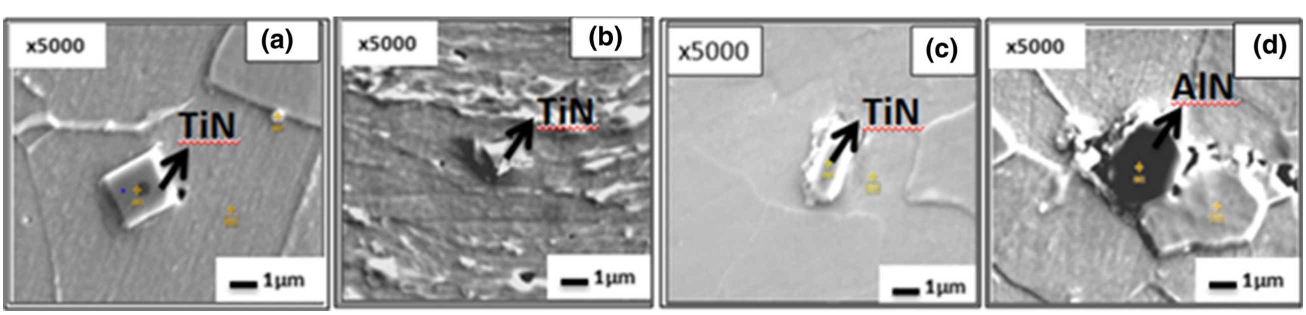


**Fig. 4** Energy dispersive spectroscopy micrographs showing presence of precipitates in **a** hot rolled **b** cold rolled **c**, **d** annealed IFHS steel

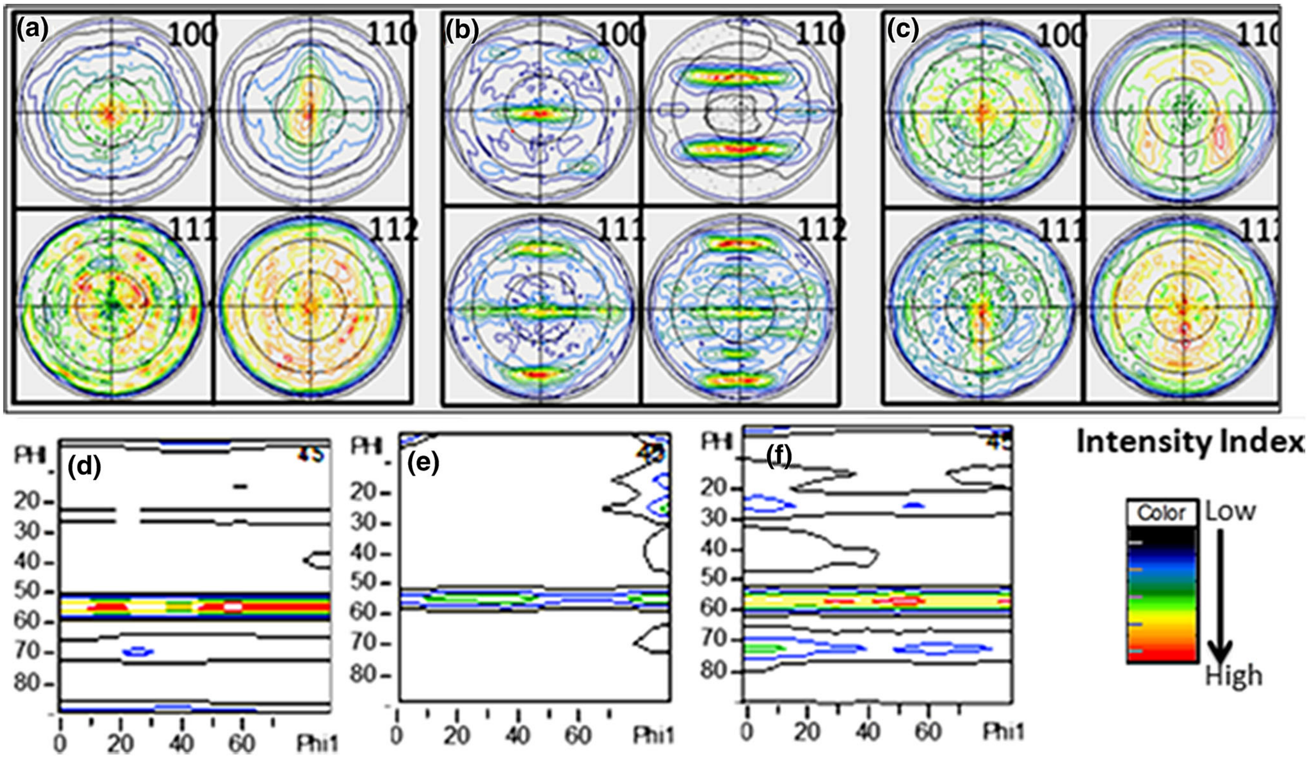


**Fig. 5** Pole figure and ODF of IFHS steel **a**, **d** hot rolled; **b**, **e** cold rolled and **c**, **f** annealed sample of IFHS respectively

In general, following conditions are said to favor the desired {111}//ND texture after annealing step [4]:

A. Finer grain sizes at the end of hot rolling;
B. Coarse precipitates in hot bands;
C. High cold reduction rate;
D. Higher annealing temperature.

During steel processing of IFHS steel, the material may either undergo a recrystallization or work hardening. These two processes lead to the formation of two primary types of textures known as recrystallization and deformation textures, respectively. Based upon the overall processing of steel, five distinct sets of texture development stages can be defined which develop during each processing step [5]:

A. Texture forming during hot rolling:
   a. First texture forming during roughing;
   b. Second texture forming during finishing;
   c. Third texture formation during controlled cooling: the gamma-to-alpha transformation;
B. Deformation texture forming during cold rolling.
C. Annealing/recrystallization texture forming after continuous annealing process.

The present paper has limited its scope in study of three textures i.e. final finish rolling texture after controlled cooling formed in hot rolling, the deformation texture formed after cold reduction and annealing texture formed after final continuous annealing treatment.

#### *3.3.1 Investigation of Hot Rolling Parameters*

The mechanical properties of hot rolled (HR) coil are a direct result of hot rolling parameters, such as rolling reduction and temperature during roughing and finishing, the controlled cooling rate at run out table before coiling. In a conventional hot rolling, the thickness of the slab is reduced to a desired hot strip thickness. In conventional hot rolling except warm rolling, the HR thickness is maintained to be lesser than 2 mm, in order to avoid uncontrolled cooling leading to mixed grain structure while strip undergo finish rolling in a two phase region.

*3.3.1.1 Reheating* Reheating temperatures when kept on a lower side, limits the coarsening of precipitates, leading to finer initial grain sizes, foremost for achieving intense textures. As such, the reheating temperatures are kept at 1020 °C in the present case. However the final textural and mechanical properties of HR coils are chiefly governed by the finishing process [5].

*3.3.1.2 Finish Rolling* The finish rolling temperature (FRT) plays pivotal role in deciding the final ferrite and the texture that evolves in hot rolled coils. The range of FRT investigated by [6] indicates that rolling in single-phase austenite rolling i.e. above 900 °C leads to a desirable fine and equiaxed ferrite structure. Such structure is desirable in terms of formability as it will produce lesser plastic anisotropic ratio ($\Delta r$) in the final structure.

The finish rolling temperature is therefore kept at 907 °C as mentioned in Table 2. If FRT is decreased below 850 °C, an undesirable coarse-grained microstructure of as-deformed ferrite is produced. It has been reported in [6] that {111}//ND is favoured either at austenitic rolling (single γ phase-field rolling) where maintained FDT during rolling is greater than 870 °C or the so called warm rolling wherein FDT is kept lower than 800 °C.

During finish rolling, larger deformations produced during interpass rolling are known to generate stronger textures facilitating favorable lattice rotation. Larger deformations not only refines the ferrite microstructure but also intensifies the high angle lattice rotations along preferred orientations.

On texture front, if the finish rolling is done in austenitic region, the resulting Ferrite structure will consist mainly of rotated cube {001}<110>, rotated goss {110}<110> and goss {110}<001> orientations with major intensity of {001}<100> orientation [5]. This is also indicated by pole figures and ODF of hot rolled steel in Fig. 5a, d.

*3.3.1.3 Coiling Through Controlled Cooling* The microstructure of the hot rolled sample as shown in Fig. 3a is subjected to a coiling temperature of 631 °C. Coiling at temperature below, 650 °C leads to formation of bimodal microstructure Fig. 3a. Coarser precipitates of TiN in the hot rolled stage can be seen in Fig. 4a. These precipitates are desirable to enhance the formability of material as they helps in development of (111) recrystallization texture [4]. Presence of TiN precipitates depicts the formation of {111)<uvw> [4]. Figure 5a, d depicting the pole figure and ODF shows the prominent texture intensity along γ-fiber at {111}<112> and {111}<011>.

### 3.3.2 *Investigation of Cold Rolling Parameters*

Very high strains are induced during cold rolling resulting in textures which can be very pronounced [7]. The bulk texture pole figure (Fig. 5b) of cold rolled material conforms to this fact showing sharp textures. These crystallographic textures lead to higher degree of anisotropy in mechanical properties of cold reduced sample shown in Table 4. This is depicted by the difference of mechanical properties (~ 100 MPa) along L and T directions (both yield and tensile strengths). During cold deformation process such as cold rolling, the dislocation pileups occur in areas of lower energy such as grains forming low angle subgrain [8].

Cold Rolling deformation process generates two fiber textures, i.e. an α-fiber texture comprising of the orientation with a common <110> direction parallel to the rolling direction (RD//<110>), while a second fiber texture, usually weak or less pronounced, is the γ-fiber comprising of the orientation {111} plane parallel to the rolling plane [9]. In the current study, α-fiber components (001) [1–10] and (111) [1–10] orientations are prominently visible as can be seen from Fig. 5e. However the absence of (114) [1–10] and (112) [1–10] depicts their weak intensity. Figure 3b shows the microstructure of the elongated grains after cold rolling. Formation of fish bone like structure depicts the formation of the in-grain bands in the microstructure. Figure 4b shows the presence of TiN.

### 3.3.3 *Investigation of Annealing Parameters*

Figure 3c shows the microstructure of the annealed sample which shows the disappearance of deformed structure and formation of small and equiaxed grains. This depicts that at the proposed annealing process parameters, complete recrystallization and grain growth occurs. Presence of TiN and AlN precipitates as shown in Fig. 4c, d in the ferrite matrix ensures the enhancement of formability, due to enhancement of {111}//ND. Banerjee [10] describes that equiaxed grains in the annealed extra deep drawing steel grade is obtained when AlN precipitates forms during coiling or after recrystallization during annealing. Equiaxed grains in the Fig. 3c indicates the formation of AlN after recrystallization during annealing which is shown in Fig. 4d as there is no evidence of any formation of AlN in the hot rolled sample as shown in Fig. 4a, d. During annealing, new grains are evolved from a cold deformed structure. The resulting new microstructure and final texture arising for the annealing process during recrystallization and subsequent grain growth is known as 'recrystallization texture' or 'annealing texture' [7] and [8].

Recrystallization process is deemed to be complete once the misorientation difference between the substructure inside and grain boundaries is within 15° and 20° and still larger misorientation between adjacent grains. This misorientation is instrumental in making grain boundaries to glide rapidly during grain growth [8]. The degree of cold deformation is instrumental in improving formability in two ways. Firstly, cold rolling induces a high dislocation density into the grains which in turn lead to recrystallization. Secondly, a higher rolling reduction greater than 75% is also known to reduce the undesirable RD-fiber [11].

During annealing process, the γ-fiber is known to be increasing whereas the α-fiber intensity decreases [11]. This is also indicated by the bulk texture (Fig. 5). The mechanism encompassing this phenomenon can be reasoned with stored energy mechanism. The stored energy mechanism for recrystallization texture proposes that since {111}<112> grains have the largest stored energy followed by the grains of the {111}<110>, {112}<110> and {001}<110> orientations respectively, it can be easily deduced that nucleation shall be preferred in {111}<112> orientation and subsequently in {111}<110> grains as described [11]. This fact can be corroborated by ODF textured figures of annealed substrate that shows peak for the above orientations (111)[1–21] and (111)[0–11]. In general, during grain growth stage, static recrystallization occurs as such; new grains are generated, further causing a decrease in the free energy and consequently a progressive increase in grain size. Hence, due to high deformation energy stored in $\gamma$-fiber orientation grains, it is the deformed grains belonging to the $\gamma$-fiber that will have preference over $\alpha$-fiber during recrystallization. In addition to this, the recovery and recrystallization time required for deformed grains of the $\alpha$-fiber is more than that of $\gamma$-fiber which leads to consumption of the former by latter fiber. Hence the recrystallization texture observed after annealing has increased $\gamma$-fiber orientations as compared to $\alpha$-fiber. Verlinden et al. [7] and Haldar et al. [12] explains the formation of $\{111\} < 110 >$ and $\{111\} < 112 >$ textures in cold rolled and annealed IFHS sheet steel. This is also depicted by pole texture figures of annealing which shows a homogeneous $\gamma$-fiber formation as indicated by low $\Delta r = 0.13$ in Table 4. Also in pole figure texture as well as in ODF representation, a weak $\alpha$-fiber also evolves.

In current study, to understand the formability behavior of IFHS steels, the approach has been guided by understanding the contribution of successive microstructural and textural transformations along with precipitation evolution occurring at various stages of steel processing. Eventually a selected set of steel processing parameters have been investigated through material characterization that contributes to formability.

## 4 Conclusions

1. The hot rolling mechanical properties as well as texture are almost similar to those obtained after annealing process. However the anisotropy is desirably decreased in latter case wherein the difference between longitudinal and transverse yield strength decreases from 25 Mpa in HR stage to 15 Mpa in annealed stage.
2. The cold rolled texture is distinctly different from both HR and CR indicating a higher degree of anisotropy with a huge difference ($\sim$100 Mpa) between longitudinal and transverse direction yield strengths.
3. The comparison of pole figures between those of HR and annealed corresponding to (111) plane shows that there is a higher degree of uniform distribution of the (111) plane aligned at 90° to the normal direction in case of Annealed in comparison to that of HR. This is also indicated by decreased anisotropy ($\Delta r = 0.13$) as well as higher formability (r bar = 1.3). One of the reasons attributing to this is a higher degree of equiaxed grain size distribution in annealed microstructure as compared to HR microstructure.
4. AlN which majorly precipitates during annealing stages may have a beneficial effect causing enhancement of $\gamma$-fiber texture by favoring (111) orientations.

## References


1. Capdevila I, Toda F G, Caballero C, Garcia-Mateo C, and de Andres CG, *Mater Sci Technol* **28** (2012) 321.
2. Kundu A, *ISIJ Int* **54** (2014) 677.
3. Lissel L, *Modeling the Microstructural Evolution during Hot Working of C–Mn and of Nb microalloyed Steels using a Physically Based Model*, Sweden (2008).
4. Ray R K, and Ghosh P, *Mater Sci Forum* **702–703** (2011) 34.
5. Butrón-Guillén M P, and Jonas J J, *ISIJ Int* **36** (1996) 68–73.
6. Ferry M, Yu D, and Chandra T, *ISIJ Int* **41** (2001) 882.
7. Verlinden B, Driver J, Samajdar I, and Doherty R D, *Thermomechanical Processing of Metallic Materials*. Pergamon Materials Series. Elsevier, Oxford (2007).
8. Castruita Ávila L G, Garcia Pastor F, and de Castro Román M J, *Matéria (Rio de Janeiro)* **20** (2015) 714–721.
9. Maruma M G, Siyasiya C W, and Stumpf W E, *J South Afr Inst Min Metall* **113** (2013) 115–120.
10. Banerjee K, *Physical Metallurgy and Drawability of Extra Deep Drawing and Interstitial Free Steels*. Intech, Rijeka, Croatia (2012). doi:10.5772/35073.
11. Nave M D, *ISIJ Int* **44** (2004) 187.
12. Haldar A, Suwas S, and Bhattacharjee D, (eds) *Microstructure texture in Steels*. Springer-Verlag, London (2009).